Supporting Information for

Recognition and Cleavage of Human tRNA Methyltransferase TRMT1 by the SARS-CoV-2 Main Protease

Angel D'Oliviera[1], Xuhang Dai[2], Saba Mottaghinia[3], Evan P. Geissler[1], Lucie Etienne[3], Yingkai Zhang[2,4], Jeffrey S. Mugridge[1]*

[1] Department of Chemistry & Biochemistry, University of Delaware, Newark, DE 19716.
[2] Department of Chemistry, New York University, New York, NY 10003.
[3] CIRI (Centre International de Recherche en Infectiologie), Univ Lyon, Inserm, U1111, Université Claude Bernard Lyon 1, CNRS, UMR5308, ENS de Lyon, F-69007 Lyon, France
[4] Simons Center for Computational Physical Chemistry at New York University, New York, NY 10003.

* Correspondence and requests for materials should be addressed to J.S.M. (email: mugridge@udel.edu)

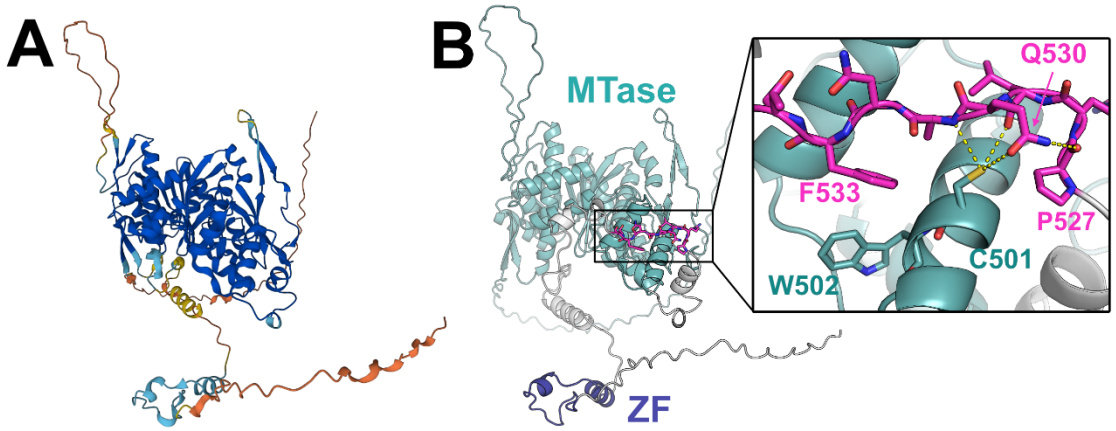

Fig. S1. AlphaFold-predicted[31,32] structure of human TRMT1. A) TRMT1 structural model colored by AlphaFold prediction confidence (dark blue = very high confidence, cyan = confident, yellow = low confidence, orange = very low confidence). B) TRMT1 structural model colored by domain (SAM-dependent methyltransferase, MTase = teal; zinc finger, ZF = cyan; linker and unstructured regions = gray) with the TRMT1(527-534) cleavage sequence highlighted in magenta. Inset shows closeup of the surface-exposed TRMT1(527-534) cleavage sequence (magenta) and the AlphaFold-predicted contacts between the residues in the cleavage sequence and the surface of the MTase domain.

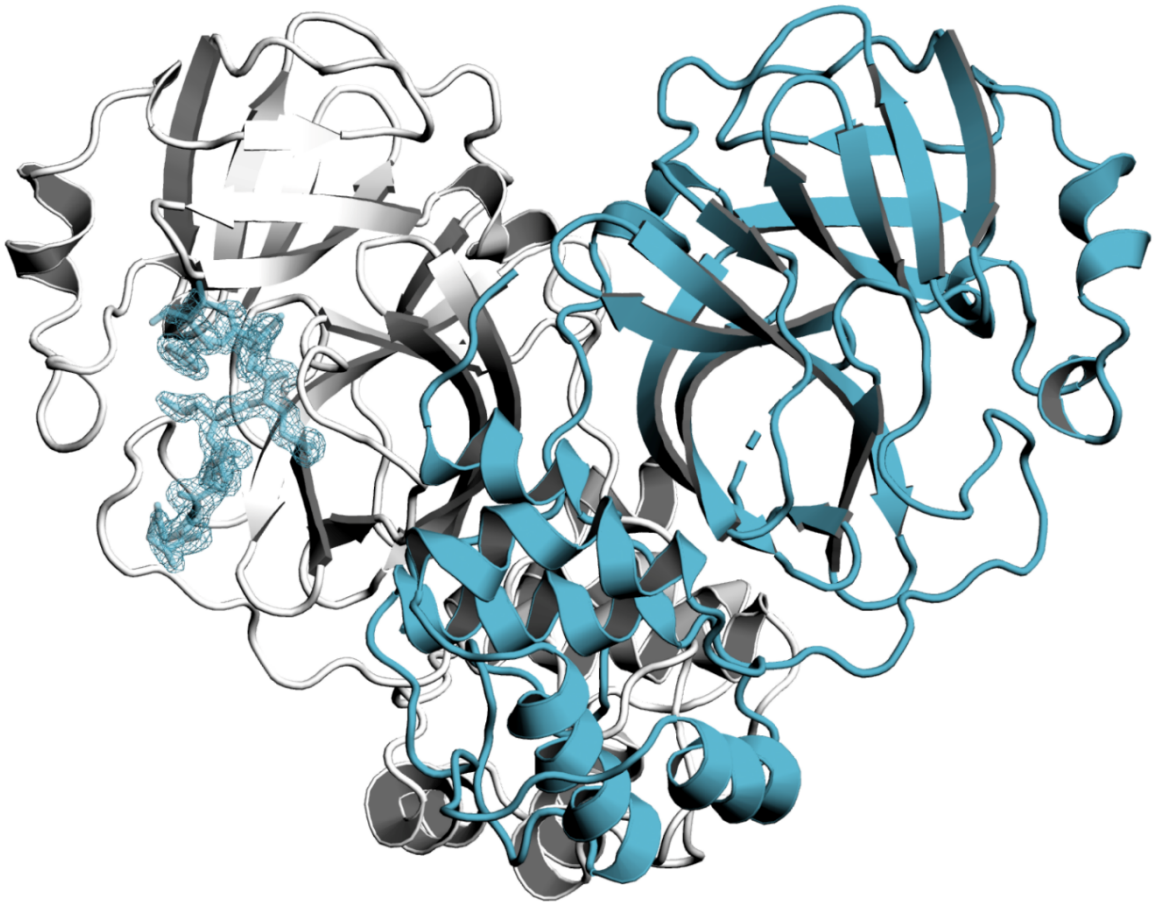

Fig. S2. Structure of human TRMT1(526-536) peptide in complex with the SARS-CoV-2 M^{pro} dimer. Only one protomer of the M^{pro} dimer has TRMT1 bound in the active site. F_o-F_c omit electron density map of TRMT1 peptide bound to M^{pro} contoured at 2σ.

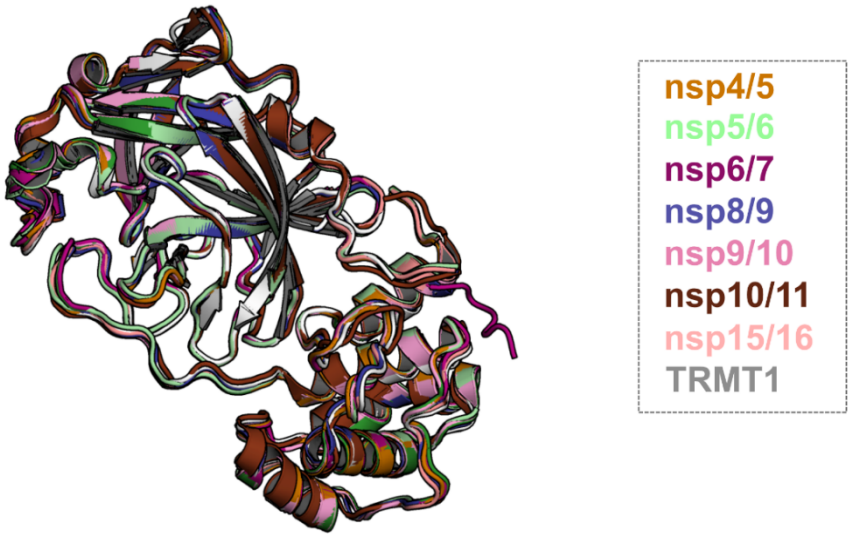

pdb	M^{pro} Mutation	Peptide Bound	Alignment RMSD
7T8M	C145A	nsp5/6	0.59
7DVX	H41A	nsp6/7	1.52
7T9Y	C145A	nsp8/9	0.75
7TA4	C145A	nsp9/10	0.70
7TA7	C145A	nsp10/11	1.07
7TC4	C145A	nsp15/16	0.53
8D35	C145A	TRMT1	0.83
7MGS	**C145A**	**nsp4/5**	**0.00**

Fig. S3. An alignment of M^{pro} structures for each M^{pro}-peptide complex used in the analysis shown in Figure 3B and C (top). Calculated all-atom RMSDs are derived from each structure alignment to M^{pro} Cys145Ala bound to nsp4/5 (7MGS) (bottom). The overall structure of the M^{pro} backbone is highly similar regardless of the bound peptide substrate.

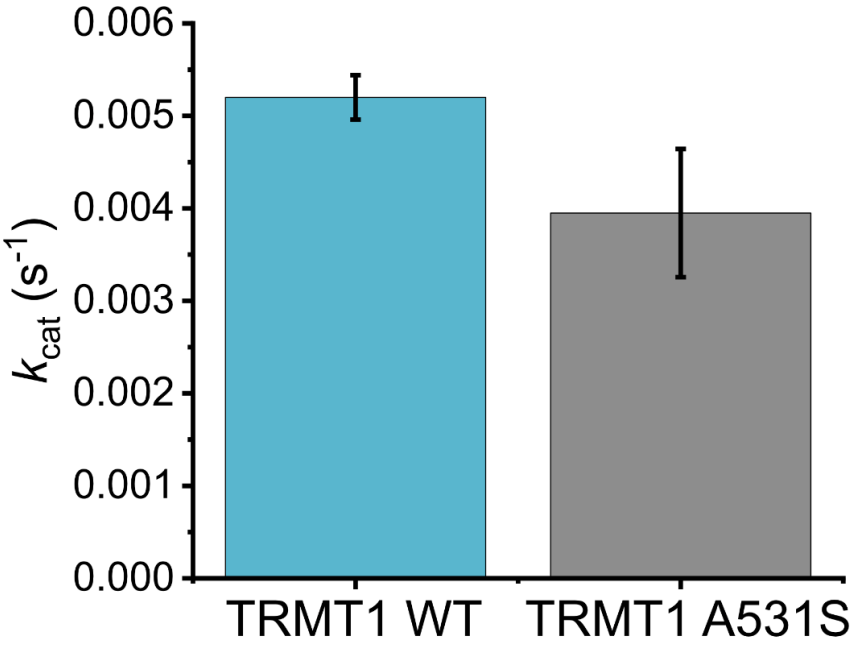

	P4	P3	P2	P1	P1′	P2′	P3′	P4′
TRMT1 WT	P	R	L	Q	A	N	F	T
TRMT1 A531S	P	R	L	Q	S	N	F	T

Fig. S4. Kinetic data comparing k_{cat} for cleavage of the TRMT1(526-536) peptide with either the WT TRMT1 sequence or an Ala531 to Ser mutation. TRMT1(A531S) contains a Ser at position P1′, which conforms to the M^{pro} cleavage consensus (Figure 1B) but is predicted to disfavor the P3′-in binding conformation observed for TRMT1 in the M^{pro} active site. No major difference is measured for cleavage of the WT vs A531S TRMT1 peptide by M^{pro}.

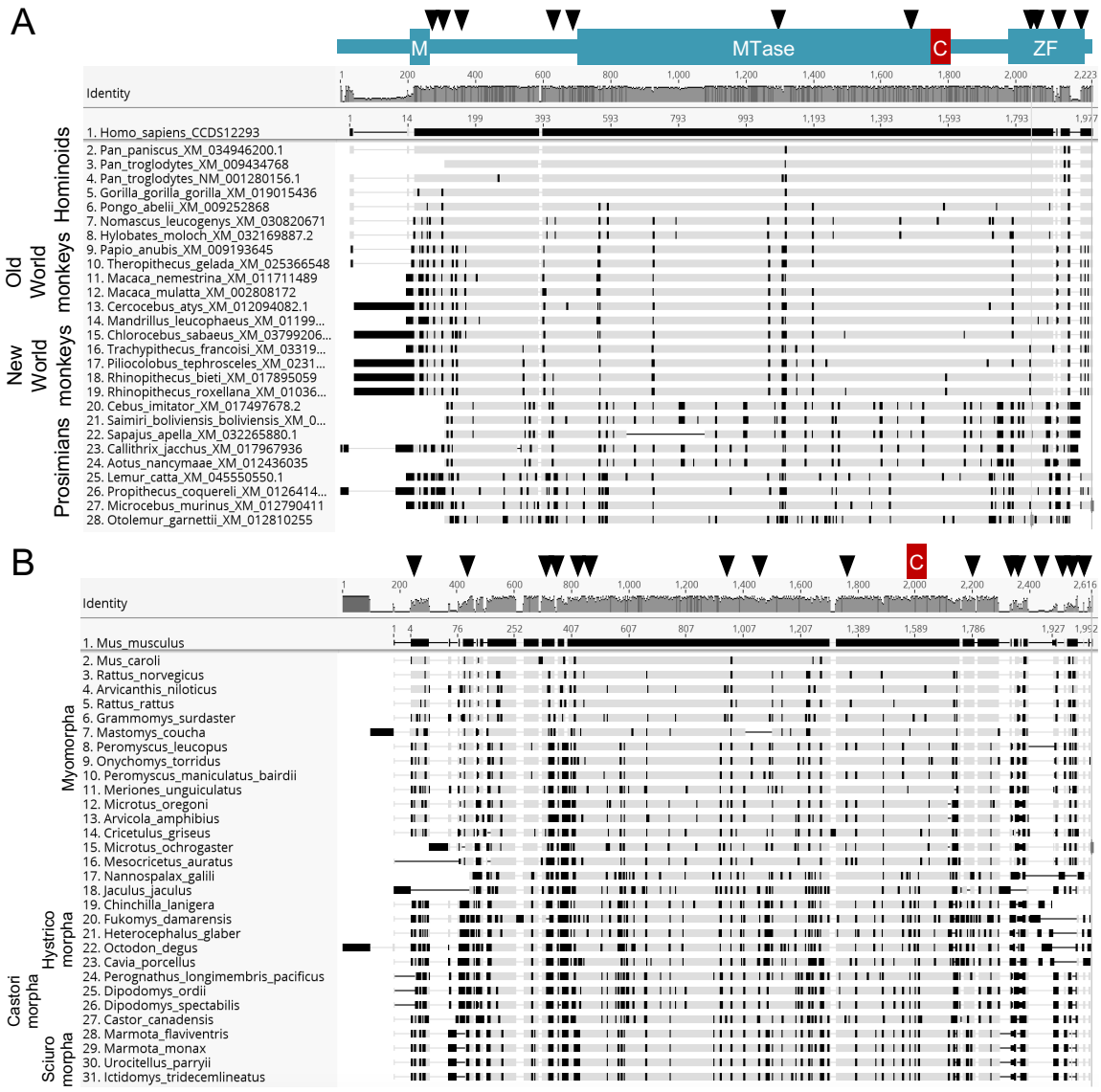

Fig. S5. Evolution of mammalian TRMT1. **A)** The M^{pro} binding/cleavage site in TRMT1 is highly conserved in primates, while there has been rapid evolution at N- and C-termini. Codon alignment of the primate TRMT1 sequences with the human as a reference. The numbering is according to the nucleotide position in the alignment (top) and in the reference sequence (human). Non-synonymous differences to the reference are highlighted in black, from Geneious R9. As indicated in Table S3, the sites under positive selection identified by MEME or FUBAR are shown above the alignment with black triangles. Major domains and the cleavage sites are also represented: M for mitochondrial signal, MTase for methyltransferase, C for cleavage by M^{pro}, ZF for Zinc finger. **B)** Same as panel A for Rodents, with mouse as the reference.

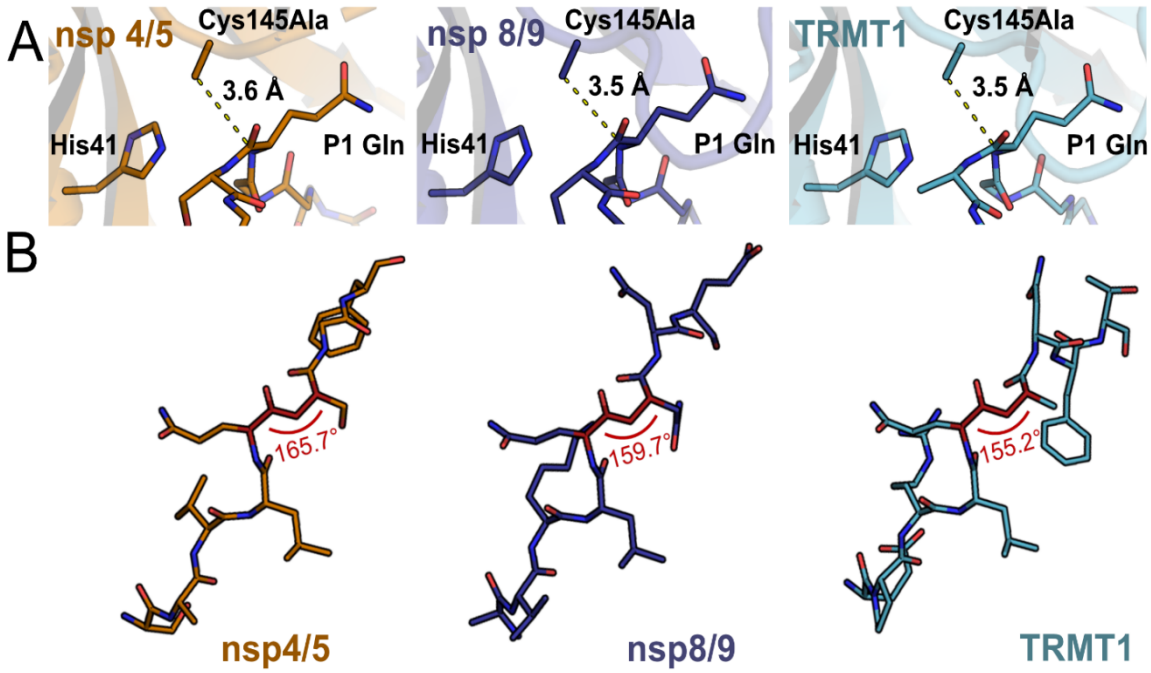

Fig. S6. Substrate positioning at the M^{pro} catalytic site does not readily explain observed differences in cleavage kinetics. **A)** One possible explanation for faster cleavage kinetics of nsp4/5 relative to nsp8/9 or TRMT1 (data in Figure 4) could be better positioning of the scissile peptide bond and electrophilic P1 amide carbonyl closer to the nucleophilic M^{pro} Cys145 residue. However, the measured C145A – P1(CO) distances are nearly identical for nsp4/5-, nsp8/9-, and TRMT1-bound M^{pro} crystal structures, suggesting this is not the case. **B)** Another possible explanation for faster cleavage kinetics of nsp4/5 are deviations in the dihedral angle of the scissile amide (P1(CA)-P1(C)-P1′(N)-P1′(CA)) bond away from 180°, which could indicate ground state destabilization that would result in accelerated peptide bond cleavage. However, the most rapidly cleaved substrate, nsp4/5, has a scissile amide bond dihedral angle closest to 180°, indicating that amide bond planarity of the bound substrate does not play an important role in determining peptide cleavage rates.

	Crystal structure of SARS-CoV-2 main protease (M^{pro}) in complex with peptide from human tRNA methyltransferase TRMT1 (PDB 8D35)
Data collection	
Space group	P 21 21 21
Cell dimensions	
a, *b*, *c* (Å)	67.79, 100.03, 103.25
α, β, γ (°)	90.00, 90.00, 90.00
Resolution (Å)	29.34 – 1.90 (1.97 – 1.90)[a]
R_{merge}	0.21 (1.75)
I / σI	9.7 (1.5)
$CC_{1/2}$	99.7 (65.6)
Completeness (%)	99.1 (98.3)
Multiplicity	13.8 (14.0)
Refinement	
Resolution (Å)	29.34 – 1.90
No. reflections	55,515 (5,407)
R / R_{free}	0.189 / 0.224
No. non-H atoms	
Protein	4719
Ligand	21
Water	359
B-factors	
Protein	30.4
Ligand	34.1
Water	37.2
R.m.s. deviations	
Bond lengths (Å)	0.007
Bond angles (°)	0.84
Ramachandran plot statistics	
No. favored	589 (98.0 %)
No. allowed	11 (1.8 %)
No. outliers	1 (0.2 %)

Data set was collected from a single crystal. [a]Values in parentheses are for highest-resolution shell.

Table S1. Data and refinement statistics for crystal structure of SARS-CoV-2 main protease (M^{pro}) in complex with peptide from human tRNA methyltransferase TRMT1 (PDB 8D35).

Substrate	M^{pro} Mutation	[M^{pro}] (μM)	k_{cat} (s^{-1})	k_{cat} +/-	K_m (μM)	K_m +/-	k_{cat}/K_m ($\mu M^{-1}s^{-1}$)	k_{cat}/K_m +/-
nsp4/5	WT	0.05	1.0492	0.04640	109	7.8	0.0097	0.00026
nsp4/5	M49A	0.05	0.4142	0.02900	75	9.6	0.0055	0.00032
nsp4/5	N142A	0.05	1.0632	0.07180	122	12.9	0.0087	0.00033
nsp4/5	Q189A	0.05	0.5274	0.10260	86	29.2	0.0061	0.00088
TRMT1	WT	0.05	0.0052	0.00024	29	3.2	0.0002	0.00001
TRMT1	M49A	0.05	0.0064	0.00030	24	2.9	0.0003	0.00002
TRMT1	N142A	0.05	0.0081	0.00038	31	3.5	0.0003	0.00002
TRMT1	Q189A	0.05	0.0062	0.00048	38	6.7	0.0002	0.00002
TRMT1(A531S)	WT	0.05	0.0040	0.00069	22	8.3	0.0002	0.00004
*nsp4/5	WT	0.25	0.5200	0.07000	41	9.0	0.0127	0.00108
*nsp8/9	WT	0.40	0.0130	0.00100	36	6.0	0.0004	0.00003

*Data from MacDonald, et al.

Table S2. Michaelis–Menten kinetics determined for different fluorogenic peptide substrates cleaved by M^{pro} wild-type (WT) and M^{pro} mutants (M49A, N142, Q189A). Individual kinetic measurements were carried out in triplicate and the +/- columns denote the standard errors on each parameter derived from non-linear least squares regression fits. *nsp4/5 and *nsp8/9 kinetic data are from MacDonald *et al*;[15] these data were measured under similar assay conditions to our nsp4/5 and TRMT1 data and our nsp4/5 kinetic parameters are in agreement for these substrates.

Dataset S1 (separate file). TRMT1 rodent and primates orthologous sequences used for evolutionary analysis and positive selection analysis of rodent and primate TRMT1 genes.

Dataset S2 (separate file). Peptide cleavage kinetic assay initial rates measured for M^{pro} WT and M^{pro} variants with nsp4/5, TRMT1, and TRMT1A531S substrates, used to determine the kinetic parameters published in this manuscript.